

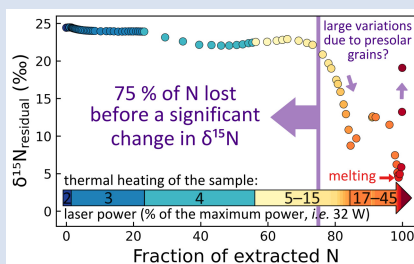
Dissecting the complex Ne-Ar-N signature of asteroid Ryugu by step-heating analysis

J. Gamblin^{1*}, E. Füri¹, B. Marty¹, L. Zimmermann¹, D.V. Bekaert¹



<https://doi.org/10.7185/geochemlet.2431>

Abstract



Samples returned from the carbonaceous asteroid (162173) Ryugu show mineralogical, chemical, and isotopic similarities with Ivuna-type (CI) carbonaceous chondrites, which likely contributed to Earth's volatile inventory. To better understand the complex Ne-Ar-N signature of CI-type material, we analysed a single, mg-sized Ryugu particle by multi-step ($n = 85$) heating. Noble gases (Ne, Ar) are a mixture between implanted Solar Wind (SW), presolar component(s), and the carbonaceous phase Q, with negligible cosmogenic contributions. The $\delta^{15}\text{N}$ variations observed during progressive heating reflect the presence of various N-bearing phases. The large number of heating steps provide key insights into the effect of thermal processing on the N abundance and isotopic ratio, and indicate that low temperatures can result in extensive N loss from CI-type material, without significantly affecting the bulk N isotopic composition. Nitrogen isotopes, therefore, remain a reliable and powerful tool for tracing volatile sources in the Solar System.

sive N loss from CI-type material, without significantly affecting the bulk N isotopic composition. Nitrogen isotopes, therefore, remain a reliable and powerful tool for tracing volatile sources in the Solar System.

Received 10 April 2024 | Accepted 25 June 2024 | Published 1 August 2024

Introduction

The Hayabusa2 mission of the Japan Aerospace Exploration Agency (JAXA) collected 5.4 g of regolith on the Cb-type asteroid (162173) Ryugu during two touchdowns in 2019 and returned the samples to Earth on December 6th, 2020 (Tsuda *et al.*, 2020). The mineralogy and the chemical and isotopic compositions of the samples revealed a close relationship between Ryugu and Ivuna-type (CI) carbonaceous chondrites (Nakamura *et al.*, 2022; Yokoyama *et al.*, 2023). However, unlike CI chondrites collected on Earth, material from Ryugu has not been affected by heating processes during atmospheric entry or by terrestrial weathering. Since carbonaceous chondrites may have played an important role in supplying volatile elements to Earth (*e.g.*, Alexander *et al.*, 2012; Marty, 2012; Alexander, 2022), Ryugu samples are key for better understanding the origin of terrestrial volatiles. The Hayabusa2-initial-analysis volatile team and the Phase-2 curation team carried out the first noble gas and N analyses, thus providing insights into the volatile composition, formation, and alteration history of Ryugu (Nakamura *et al.*, 2022; Okazaki *et al.*, 2023). The noble gases were found to be mainly primordial (*i.e.* carried by the so called phase Q and a variety of presolar components), with variable contributions from solar wind (SW) and cosmogenic isotopes. Okazaki *et al.* (2023) concluded that the heterogeneous N contents and isotopic compositions of Ryugu samples, including four small pelletised samples and three splits of a large aggregate sample (Naraoka *et al.*, 2023), indicate the presence of at least two carrier phases: a N-rich phase with $\delta^{15}\text{N}$ up to +70 ‰ and a N-depleted phase with $\delta^{15}\text{N}$ near 0 ‰. These results were subsequently discussed in more detail by Broadley *et al.* (2023) and Hashizume *et al.* (2024).

Here, we aim to better understand the nature and behaviour of Ne-Ar-N carriers in Ryugu material by performing a large number ($n = 85$) of extraction steps at incrementally increasing temperature. This is the first time, to our knowledge, that a single asteroidal particle has been heated in so many steps for coupled noble gas and N analyses, thereby providing unprecedented insight into the complex Ne-Ar-N makeup of primitive extraterrestrial matter.

Material and Methods

Particle C0015 (1.8 ± 0.2 mg), collected during the second touchdown on Ryugu within a crater created by the spacecraft's small carry-on impactor, was targeted for step-heating Ne-Ar-N analysis at the Centre de Recherches Pétrographiques et Géo-chimiques (CRPG) noble gas facility. The particle was never in contact with Earth's atmosphere and was constantly kept within a dry N_2 atmosphere or under vacuum during sample preparation, storage, and analysis. The particle was heated under static vacuum using a CO_2 laser at increasing laser power, and the fraction of noble gases (Ne, Ar) and N (in the form of N_2) extracted at each step was analysed using a Noblesse-HR noble gas mass spectrometer in multi-collection. A total of 85 heating steps were performed to study the progressive release of different noble gas and N components. Details on the analytical procedure and data treatment are provided in the Supplementary Information.

Ne-Ar-N Release Patterns of Particle C0015

Figure 1 shows the release patterns of Ne, Ar, and N (analysed in the form of N_2) and the corresponding isotope ratios measured

1. Université de Lorraine, CNRS, CRPG, F-54000 Nancy, France

* Corresponding author (email: julie.gamblin@univ-lorraine.fr)

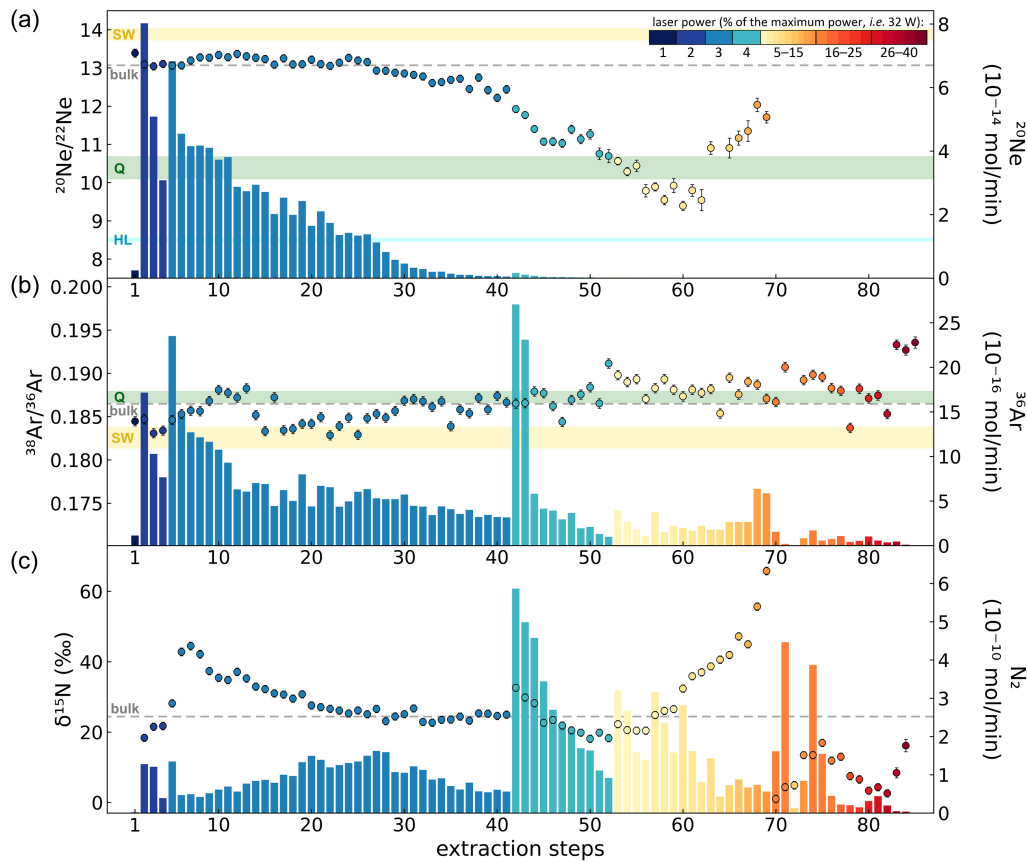


Figure 1 (a) ^{20}Ne , (b) ^{36}Ar , and (c) N_2 abundances (filled bars) and isotope ratios (filled circles) of particle C0015 for 85 extraction steps. Abundances are weighted by the extraction duration (*i.e.* 4 min for the first 26 steps and 12 min for the following 59 steps). Isotope ratios are shown for heating steps with $<30\%$ blank contributions. The different colours represent the laser power used for the extraction (*i.e.* 1 to 45 % of the total power of 32 W). The dashed lines indicate the calculated “bulk” $^{20}\text{Ne}/^{22}\text{Ne}$, $^{38}\text{Ar}/^{36}\text{Ar}$, and $\delta^{15}\text{N}$ values. Isotope ratios of the solar wind (SW), phase Q, and Ne-HL are shown for comparison (see Ott, 2014 and references therein). Uncertainties are 1σ and error bars are, in most cases, smaller than symbol sizes.

at each heating step. Most of the Ne was released at very low laser power ($\leq 3\%$) at which the camera view showed no visible heating (indicated by an orange glow) of the particle. The $^{20}\text{Ne}/^{22}\text{Ne}$ ratio was nearly constant (12.92 ± 0.47) during the first 38 extraction steps (Fig. 1a), only slightly below the Ne isotope ratio of SW (13.74 ± 0.02 to 14.00 ± 0.04 ; Ott, 2014) and close to that of the protosolar nebula (~ 13.36 ; Heber *et al.*, 2012). This plateau likely results from the extraction of a pure Ne component. While trapping of nebular gas in CI-type material cannot be ruled out, the $^3\text{He}/^4\text{He}$ ratio of solar-gas-rich Ryugu samples analysed previously is consistent with implanted SW-derived gas (Meshik *et al.*, 2023; Okazaki *et al.*, 2023). Neon released at low temperatures must, therefore, be predominantly derived from the SW, fractionated to an isotopically lighter value upon implantation and grain surface sputtering (Grimberg *et al.*, 2006). At higher temperatures, the $^{20}\text{Ne}/^{22}\text{Ne}$ ratio first decreased significantly to 9.39 ± 0.12 , before increasing to 12.03 ± 0.18 . Since the $^{21}\text{Ne}/^{22}\text{Ne}$ ratio varied only between ~ 0.026 and 0.049 (Fig. 2), which implies a small proportion of cosmogenic Ne (*i.e.* $<0.1\%$ $^{21}\text{Ne}_{\text{cosm}}$) in particle C0015, the $^{20}\text{Ne}/^{22}\text{Ne}$ variations are inferred to predominantly reflect the release of the primordial components Ne-Q and Ne-HL. The Ne amounts released during the last 15 steps were too low for reliable isotope ratio measurements. The results indicate the presence of at least three Ne components in Ryugu particle C0015: SW-derived Ne implanted at the grain surface, Ne-HL carried by presolar nanodiamonds, and Ne-Q (or P1) carried by phase Q (Fig. 2b). Overall, the Ne composition of particle

C0015 is dominated by the SW component (Fig. 2a), similar to two pellets studied by the Hayabusa2-initial-analysis volatile team (Okazaki *et al.*, 2023) and several particles analysed by the Phase-2 curation team (Nakamura *et al.*, 2022).

The ^{40}Ar signal was small for steps #2 and #5, and comparable to the blank value throughout the rest of the heating procedure, demonstrating the absence of any adsorbed atmospheric Ar. The $^{38}\text{Ar}/^{36}\text{Ar}$ ratio of the Ar fraction released at low laser power first oscillated between the Ar-SW (0.1818 ± 0.0005 to 0.1828 ± 0.0010 ; Ott, 2014) and Ar-Q values (0.1872 ± 0.0007 ; Wieler *et al.*, 1992), then plateaued around Ar-Q (Fig. 1b). Ar-HL (0.227 ± 0.003 ; Ott, 2014), expected to be released from presolar diamonds at relatively low temperatures (Supplementary Information), likely also contributed to the observed variations. Unlike Ne, a large amount of Ar was released at higher temperatures, implying that a significant proportion of Ar in particle C0015 was carried by refractory phases. The elevated $^{38}\text{Ar}/^{36}\text{Ar}$ ratios observed during sample melting (*i.e.* after step #80, at $\geq 24\%$ laser power) can be explained by a very small contribution of cosmogenic ^{38}Ar ($(^{38}\text{Ar}/^{36}\text{Ar})_{\text{cosm}} \sim 1.54$; Wieler, 2002). The calculated bulk $^{38}\text{Ar}/^{36}\text{Ar}$ ratio (0.1865 ± 0.0001 ; Table S-1) is comparable to that of Ar-Q and similar to the values previously reported for Ryugu (0.186 ± 0.001 to 0.194 ± 0.007 ; Okazaki *et al.*, 2023).

The amount of N released and the corresponding $\delta^{15}\text{N}$ varied significantly for the different extraction steps, reflecting the presence of several, isotopically distinct N components in Ryugu material. The blank contribution exceeded 30 % of the

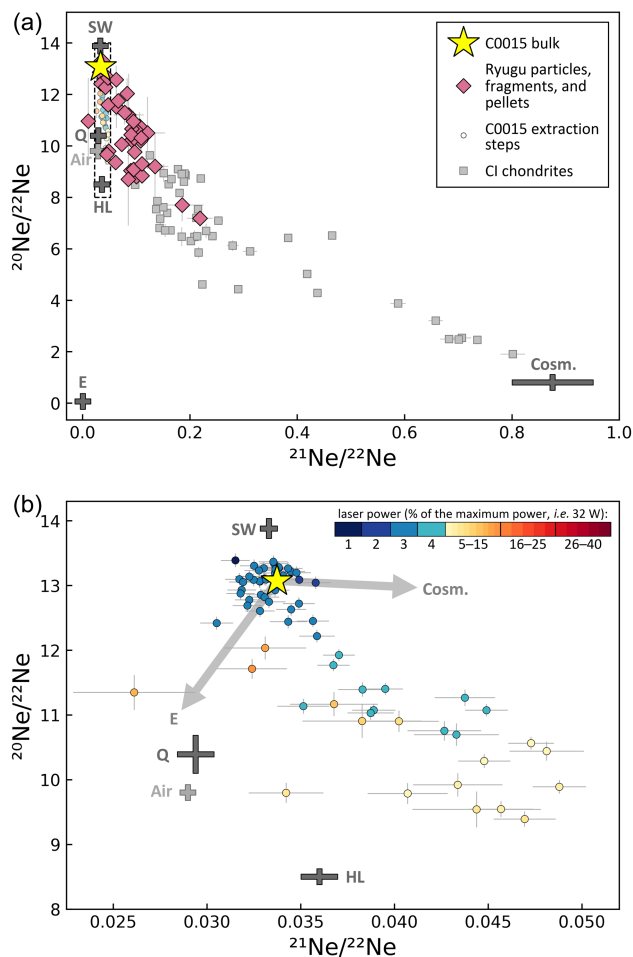


Figure 2 (a) Neon isotopic composition of Ryugu particle C0015 (bulk represented by the yellow star; individual extraction steps represented by the small circles) compared to pelletised and fragment Ryugu samples analysed by the Hayabusa2-initial-analysis volatile team and particles analysed by the Phase-2 curation team (Institute for Planetary Materials, Okayama University) (pink diamonds), as well as CI chondrites (grey squares) (Nakamura *et al.*, 2022; Broadley *et al.*, 2023; Meshik *et al.*, 2023; Okazaki *et al.*, 2023 and references therein). Different Ne end members are represented by grey crosses (Ott, 2014). Ne-E is mainly carried by presolar graphite and silicon carbide. (b) Close-up (corresponding to the dashed rectangle in panel (a)) of the Ne isotopic variations observed for the 85 extraction steps of particle C0015. The different colours represent the laser power used for each extraction. Uncertainties are 1σ .

measured N_2 signal at step #1, and a $\delta^{15}N$ of $+18.4 \pm 1.0$ ‰ was measured at step #2. This indicates that the contribution of any dry N_2 adsorbed onto the sample surface during sample storage and handling must be negligible, provided that this component is characterised by an atmospheric isotope signature. Whereas the $\delta^{15}N$ ranged from $+18.1 \pm 1.0$ up to $+44.5 \pm 1.1$ ‰ during the first 52 steps (*i.e.* at a low laser power, ≤ 4 %), $\delta^{15}N$ increased to $+65.8 \pm 1.1$ ‰ at step #69 and then suddenly dropped to $+1.0 \pm 1.0$ ‰ at step #70. No clear SW contribution ($\delta^{15}N_{SW} = -407 \pm 7$ ‰; Marty *et al.*, 2011) could be identified, even for low temperature extraction steps. Thus, the N release pattern is clearly decoupled from that of Ne. Assuming an unfractionated SW $^{20}Ne/^{14}N$ elemental abundance ratio of 1.14 (Marty *et al.*, 2010), any SW-derived N is indeed expected to be undetectable in the ^{20}Ne -rich particle C0015.

The production of cosmogenic ^{15}N during exposure to cosmic rays can potentially modify the N isotope ratio of

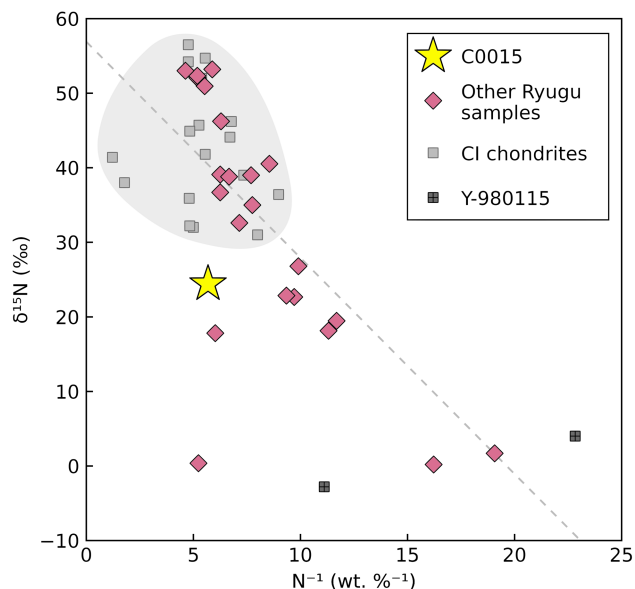


Figure 3 Nitrogen isotopic composition ($\delta^{15}N$) as a function of the inverse of the N concentration of Ryugu samples compared to CI chondrites and Y-980115, a CI chondrite recovered in Antarctica that has recently been recommended to be re-classified as a Yamato-type (CY) carbonaceous chondrite (King *et al.*, 2019). Adapted from Okazaki *et al.* (2023) and Hashizume *et al.* (2024), including data reported in Table S-2. A simple two-component mixture, between a N-rich phase with $\delta^{15}N$ up to $+70$ ‰ and a N-depleted phase with $\delta^{15}N$ near 0 ‰, fails to explain the N signature of Ryugu particle C0015.

extraterrestrial samples. Combined analyses of noble gases and N make it possible to quantify the amount of $^{15}N_{cosm}$ and to identify the isotopic composition of primordial N. Previous Ne analyses revealed that Ryugu samples record short cosmic ray exposure (CRE) ages of ~ 100 kyr to 8 Myr (Nakamura *et al.*, 2022; Okazaki *et al.*, 2023). The Ne isotopic composition of particle C0015 studied here closely resembles that of pellets A0105-15 and A0105-06, which are dominated by Ne-SW and contain a negligible amount of cosmogenic Ne. By using the same $^{21}Ne_{cosm}$ production rate as Okazaki *et al.* (2023) (*i.e.* $P_{21} = 1.34 \times 10^{-13}$ mol g^{-1} Myr $^{-1}$), together with a simplified one-stage irradiation model, the CRE age of particle C0015 is estimated at $\sim 30,000$ years. This exposure duration could result in the production of $\sim 4 \times 10^{-17}$ mol ^{15}N (when using the maximum $(^{15}N/^{21}Ne)_{cosm} = 5.5$ from Mathew and Murty, 1993, estimated for H/L chondrites), which is negligible compared to the bulk N content of the sample. Since particle C0015 has neither been measurably affected by the production of cosmogenic ^{15}N nor atmospheric contamination and N-SW implantation, it preserves key information on N components and carrier phases in Ryugu and CI-type material. However, distinguishing between different labile and more refractory N components in particle C0015 is challenging because, in contrast to the noble gases, the nature and N isotope compositions of potential chondritic N carrier phases are highly complex, as detailed in the Supplementary Information. While the different N carrier phases cannot be deciphered, the observed N release pattern (Fig. 1c) and the summed bulk N signature (Fig. 3) require the presence of more than just two N components, in contrast to previous findings of Okazaki *et al.* (2023) and Hashizume *et al.* (2024).

Discussion

The mineralogical, chemical, and isotopic characteristics of Ryugu revealed a close relationship with CI-chondrites

(Nakamura *et al.*, 2022; Yokoyama *et al.*, 2023). The CI group nominally comprises the five falls Orgueil, Alais, Ivuna, Tonk, and Revelstoke, whose bulk N isotopic compositions vary between +31 and +61 ‰ (based on analyses of Alais, Ivuna, and Orgueil; Table S-2 and references therein) (Fig. 3). It is noteworthy that the Meteoritical Bulletin lists an additional four CIs that were recovered in the Yamato Mountains in Antarctica (Y-86029, Y-86737, Y-980115, and Y-980134), two of which (Y-86029 and Y-980115) have been recommended to be re-classified as Yamato-type (CY) chondrites (King *et al.*, 2019). The bulk $\delta^{15}\text{N}$ of Y-980115 was reported to vary from -2.8 ‰ to $+4.0$ ‰ (Chan *et al.*, 2016; Hashizume *et al.*, 2024) (Fig. 3), distinct from the CI signature.

The N abundances and isotopic compositions of several particles collected at Ryugu's surface (Ryugu-A samples) or within an artificial crater (Ryugu-C samples) fall within the CI range; however, some samples show lower N contents and/or $\delta^{15}\text{N}$ values (Fig. 3; Nakamura *et al.*, 2022; Broadley *et al.*, 2023; Naraoka *et al.*, 2023; Oba *et al.*, 2023; Hashizume *et al.*, 2024). The four pelleted samples analysed by the Hayabusa2-initial-analysis volatile team have particularly low N contents (Table S-2). The bulk $\delta^{15}\text{N}$ of $+24.43 \pm 0.17$ ‰ of particle C0015 (Table S-1) is comparable to the values previously obtained for the pellets A0105-05 and C0106-06 by noble gas mass spectrometry at CRPG ($+18.14 \pm 0.94$ ‰ and $+19.47 \pm 0.89$ ‰; Broadley *et al.*, 2023; Okazaki *et al.*, 2023), whereas its summed bulk N abundance (1760 ± 195 ppm; Table S-1) is consistent with the range observed in most CI chondrites (1400 to 2400 ppm; Table S-2 and references therein). Notably, particle C0015 contains more Ne and Ar than CI chondrites ($^{36}\text{Ar} = 4.33 \pm 2.78 \times 10^{-11}$ mol/g and $^{20}\text{Ne} = 1.53 \pm 0.03 \times 10^{-11}$ mol/g, on average, in CIs; Broadley *et al.*, 2023 and references therein), but the large noble gas abundance predominantly results from SW irradiation.

Broadley *et al.* (2023) suggested that preferential loss of ^{15}N -rich soluble organic matter during aqueous alteration on Ryugu's parent body may have resulted in a lower $\delta^{15}\text{N}$ and lower N concentrations in Ryugu samples than in CIs, without significantly affecting the noble gas budget. According to this scenario, the N heterogeneities between the various small, (sub-)milligram-sized Ryugu samples could be due to variable degrees of aqueous alteration on the initial parent body, prior to the catastrophic break-up that turned Ryugu into a rubble-pile asteroid and led to mixing between more and less altered clasts (Broadley *et al.*, 2023). However, this process alone can neither explain the association of "intermediate" $\delta^{15}\text{N}$ values with high N abundances in particles C0015 (this study) and A0033 (Nakamura *et al.*, 2022), nor the very low $\delta^{15}\text{N}$ value and high N content of particle C0082 (Nakamura *et al.*, 2022) (Fig. 3). Significant heterogeneities of the N distribution must, therefore, exist at the scale of (sub-)milligram-sized Ryugu regolith particles, as also demonstrated by *in situ* secondary ion mass spectrometry analyses of N (Nakamura *et al.*, 2022).

CI-type material is inferred to have played an important role in supplying volatile elements (*e.g.*, H, C, N) to Earth's surface (Piani *et al.*, 2020). However, since thermal metamorphism and accretionary heating could have resulted in extensive devolatilisation and loss of ^{15}N -rich components (Alexander *et al.*, 1998, Alexander *et al.*, 2007; Pearson *et al.*, 2006; Grewal, 2022), assessing the evolution of the N content and isotopic composition during progressive heating is key for understanding the contribution of CIs to Earth's volatile budget. The numerous heating steps performed on Ryugu particle C0015 provide key information on N abundance and isotopic variations induced by thermal processing, especially since Ryugu never experienced temperatures >150 °C (based on analyses of soluble organic

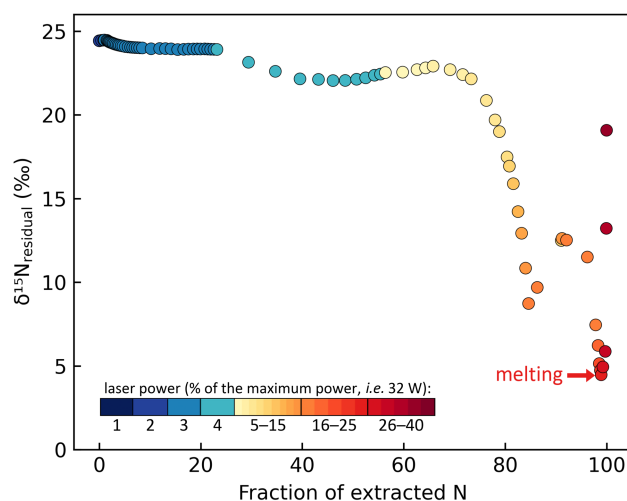


Figure 4 Evolution of the residual N isotopic composition ($\delta^{15}\text{N}_{\text{residual}}$) of particle C0015 as a function of the fraction of N extracted by progressive heating.

matter in Ryugu; Naraoka *et al.*, 2023). Figure 4 illustrates that the "bulk" $\delta^{15}\text{N}$ value of particle C0015 was not significantly modified during the first 60 heating steps (*i.e.* $\delta^{15}\text{N} = 22.05 \pm 0.22$ ‰ to 24.47 ± 0.17 ‰ for 1 to 7 % of the maximum laser power), although up to ~ 73 % of the total initial N content was lost. As heating proceeded and particle C0015 started to melt at step #80, the $\delta^{15}\text{N}$ decreased to 4.47 ± 0.47 ‰ (with concomitant loss of ~ 99 % N). This observation confirms that Ryugu samples contain a refractory N component with an isotopic composition similar to Earth's atmosphere (Hashizume *et al.*, 2024) whose proportion of the total amount of N, however, is very small.

Overall, N-rich material collected at Ryugu's surface is predominantly characterised by an isotopic signature that is comparable to, or only slightly lighter than, that of CI chondrites ($\delta^{15}\text{N} \geq +18$ ‰; Fig. 3; Table S-2). Furthermore, our new data demonstrate that low temperatures can result in extensive N loss from CI-type material, without significantly affecting the bulk N isotope composition. Only high temperatures result in loss of a ^{15}N -rich component and a notable decrease of the bulk $\delta^{15}\text{N}$ value by ~ 20 ‰. Consequently, and despite potential losses of thermally labile N-bearing phases, N isotopes remain a reliable and powerful tool for tracing contributions from inner and outer Solar System sources, and they imply that CI- or Ryugu-type material can be ruled out as the major source of N in Earth's mantle.

Acknowledgements

The Hayabusa2 mission was developed under the leadership of the Japan Aerospace Exploration Agency (JAXA), with contributions from the German Aerospace Center (DLR) and the Centre National d'Études Spatiales (CNES), and in collaboration with NASA, and other universities and institutes. This work was primarily funded by the European Union (ERC, IRONIS, 101087562). Views and opinions expressed are however those of the author(s) only and do not necessarily reflect those of the European Union or the European Research Council. Neither the European Union nor the granting authority can be held responsible for them. Support from the Centre National d'Études Spatiales (CNES) is also acknowledged. We thank Michael W. Broadley for his help with handling the Hayabusa2 samples as well as Bouchaib Tibari and Allan

Bauer for their assistance with the noble gas mass spectrometry analyses at CRPG. We are also grateful to R. Wieler, C.M.O'D. Alexander, and an anonymous reviewer for their constructive comments, and to A. Shahar for editorial handling. This is CRPG contribution 2858.

Editor: Anat Shahar

Additional Information

Supplementary Information accompanies this letter at <https://www.geochemicalperspectivesletters.org/article2431>.



© 2024 The Authors. This work is distributed under the Creative Commons Attribution Non-Commercial No-Derivatives 4.0

License, which permits unrestricted distribution provided the original author and source are credited. The material may not be adapted (remixed, transformed or built upon) or used for commercial purposes without written permission from the author. Additional information is available at <https://www.geochemicalperspectivesletters.org/copyright-and-permissions>.

Cite this letter as: Gamblin, J., Füre, E., Marty, B., Zimmermann, L., Bekaert, D.V. (2024) Dissecting the complex Ne-Ar-N signature of asteroid Ryugu by step-heating analysis. *Geochem. Persp. Let.* 31, 44–48. <https://doi.org/10.7185/geochemlet.2431>

References

- ALEXANDER, C.M.O'D. (2022) An exploration of whether Earth can be built from chondritic components, not bulk chondrites. *Geochimica et Cosmochimica Acta* 318, 428–451. <https://doi.org/10.1016/j.gca.2021.12.012>
- ALEXANDER, C.M.O'D., RUSSELL, S.S., ARDEN, J.W., ASH, R.D., GRADY, M.M., PILLINGER, C.T. (1998) The origin of chondritic macromolecular organic matter: A carbon and nitrogen isotope study. *Meteoritics & Planetary Science* 33, 603–622. <https://doi.org/10.1111/j.1945-5100.1998.tb01667.x>
- ALEXANDER, C.M.O'D., FOGEL, M., YABUTA, H., CODY, G.D. (2007) The origin and evolution of chondrites recorded in the elemental and isotopic compositions of their macromolecular organic matter. *Geochimica et Cosmochimica Acta* 71, 4380–4403. <https://doi.org/10.1016/j.gca.2007.06.052>
- ALEXANDER, C.M.O'D., BOWDEN, R., FOGEL, M.L., HOWARD, K.T., HERD, C.D.K., NITTLER, L.R. (2012) The provenances of asteroids, and their contributions to the volatile inventories of the terrestrial planets. *Science* 337, 721–723. <https://doi.org/10.1126/science.1223474>
- BROADLEY, M.W., BYRNE, D.J., FÜRER, E., ZIMMERMANN, L., MARTY, B. *et al.* (2023) The noble gas and nitrogen relationship between Ryugu and carbonaceous chondrites. *Geochimica et Cosmochimica Acta* 345, 62–74. <https://doi.org/10.1016/j.gca.2023.01.020>
- CHAN, Q.H.S., CHIKARAISHI, Y., TAKANO, Y., OGAWA, N.O., OHKOUCHI, N. (2016) Amino acid compositions in heated carbonaceous chondrites and their compound-specific nitrogen isotopic ratios. *Earth, Planets and Space* 68, 7. <https://doi.org/10.1186/s40623-016-0382-8>
- GREWAL, D.S. (2022) Origin of nitrogen isotopic variations in the rocky bodies of the solar system. *The Astrophysical Journal* 937, 123. <https://doi.org/10.3847/1538-4357/ac8eb4>
- GRIMBERG, A., BAUER, H., BOCHSLER, P., BÜHLER, F., BURNETT, D.S., HAYS, C.C., HEBER, V.S., JUREWICZ, A.J.G., WIELER, R. (2006) Solar wind neon from Genesis: implications for the lunar noble gas record. *Science* 317, 1133–1135. <https://doi.org/10.1126/science.1133568>
- HASHIZUME, K., ISHIDA, A., CHIBA, A., OKAZAKI, R., YOGATA, K., YADA, T., KITAJIMA, F., YURIMOTO, H., NAKAMURA, T., NOGUCHI, T., YABUTA, H., NARAOKA, H., TAKANO, Y., SAKAMOTO, K., TACHIBANA, S., NISHIMURA, M., NAKATO, A., MIYAZAKI, A., ABE, M., OKADA, T., USUI, T., YOSHIKAWA, M., SAIKI, T., TERUI, F., TANAKA, S., NAKAZAWA, S., WATANABE, S.-I., TSUDA, Y., BROADLEY, M.W., BUSEMANN, H., HAYABUSA2 INITIAL ANALYSIS VOLATILE TEAM (2024) The Earth atmosphere-like bulk nitrogen isotope composition obtained by stepwise combustion analyses of Ryugu return samples. *Meteoritics & Planetary Science*. <https://doi.org/10.1111/maps.14175>
- HEBER, V.S., BAUR, H., BOCHSLER, P., MCKEEGAN, K.D., NEUGEBAUER, M., REISENFELD, D.B., WIELER, R., WIENS, R.C. (2012) Isotopic mass fractionation of solar wind: evidence from fast and slow solar wind collected by the Genesis mission. *The Astrophysical Journal* 759, 121. <https://doi.org/10.1088/0004-637X/759/2/121>
- KING, A.J., BATES, H.C., KRIETSCH, D., BUSEMANN, H., CLAY, P.L., SCHOFIELD, P.F., RUSSELL, S.S. (2019) The Yamato-type (CY) carbonaceous chondrite group: Analogues for the surface of asteroid Ryugu? *Geochemistry* 79, 125531. <https://doi.org/10.1016/j.chemer.2019.08.003>
- MARTY, B. (2012) The origins and concentrations of water, carbon, nitrogen and noble gases on Earth. *Earth and Planetary Science Letters* 313–314, 56–66. <https://doi.org/10.1016/j.epsl.2011.10.040>
- MARTY, B., ZIMMERMANN, L., BURNARD, P.G., WIELER, R., HEBER, V.S., BURNETT, D.S., WIENS, R.C., BOCHSLER, P. (2010) Nitrogen isotopes in the recent solar wind from the analysis of Genesis targets: Evidence for large scale isotope heterogeneity in the early solar system. *Geochimica et Cosmochimica Acta* 74, 340–355. <https://doi.org/10.1016/j.gca.2009.09.007>
- MARTY, B., CHAUSSIDON, M., WIENS, R.C., JUREWICZ, A.J.G., BURNETT, D.S. (2011) A ¹⁵N-poor isotopic composition for the solar system as shown by Genesis solar wind samples. *Science* 332, 1533–1536. <https://doi.org/10.1126/science.1204656>
- MATHEW, K.J., MURTY, S.V.S. (1993) Cosmic ray produced nitrogen in extra terrestrial matter. *Journal of Earth System Science* 102, 415–437. <https://doi.org/10.1007/BF02841731>
- MESHIK, A., PRAVDIVTSEVA, O., OKAZAKI, R., YOGATA, K., YADA, T. *et al.* (2023) Noble gas mass-spectrometry for extraterrestrial micro-samples: analyses of asteroid matter returned by Hayabusa2 JAXA mission. *Journal of Analytical Atomic Spectrometry* 38, 1785–1797. <https://doi.org/10.1039/D3JA00125C>
- NAKAMURA, E., KOBAYASHI, K., TANAKA, R., KUNIHIRO, T., KITAGAWA, H. *et al.* (2022) On the origin and evolution of the asteroid Ryugu: A comprehensive geochemical perspective. *Proceedings of the Japan Academy, Series B* 98, 227–282. <https://doi.org/10.2183/pjab.98.015>
- NARAOKA, H., TAKANO, Y., DWORIN, J.P., OBA, Y., HAMASE, K. *et al.* (2023) Soluble organic molecules in samples of the carbonaceous asteroid (162173) Ryugu. *Science* 379, eabn9033. <https://doi.org/10.1126/science.abn9033>
- OBA, Y., KOGA, T., TAKANO, Y., OGAWA, N.O., OHKOUCHI, N. *et al.* (2023) Uracil in the carbonaceous asteroid (162173) Ryugu. *Nature Communications* 14, 1292. <https://doi.org/10.1038/s41467-023-36904-3>
- OKAZAKI, R., MARTY, B., BUSEMANN, H., HASHIZUME, K., GILMOUR, J.D. *et al.* (2023) Noble gases and nitrogen in samples of asteroid Ryugu record its volatile sources and recent surface evolution. *Science* 379, eabo431. <https://doi.org/10.1126/science.abo431>
- OTT, U. (2014) Planetary and pre-solar noble gases in meteorites. *Geochemistry* 74, 519–544. <https://doi.org/10.1016/j.chemer.2014.01.003>
- PEARSON, V.K., SEPTON, M.A., FRANCHI, I.A., GIBSON, J.M., GILMOUR, I. (2006) Carbon and nitrogen in carbonaceous chondrites: Elemental abundances and stable isotopic compositions. *Meteoritics & Planetary Science* 41, 1899–1918. <https://doi.org/10.1111/j.1945-5100.2006.tb00459.x>
- PIANI, L., MARROCCHI, Y., RIGAUDIER, T., VACHER, L.G., THOMASSIN, D., MARTY, B. (2020) Earth's water may have been inherited from material similar to enstatite chondrite meteorites. *Science* 369, 1110–1113. <https://doi.org/10.1126/science.aba1948>
- TSUDA, Y., SAIKI, T., TERUI, F., NAKAZAWA, S., YOSHIKAWA, M., WATANABE, S. (2020) Hayabusa2 mission status: Landing, roving and cratering on asteroid Ryugu. *Acta Astronautica* 171, 42–54. <https://doi.org/10.1016/j.actaastro.2020.02.035>
- WIELER, R. (2002) Cosmic-ray-produced noble gases in meteorites. In: PORCELLI, D., BALLENTINE, C., WIELER, R. (Eds.) *Reviews in Mineralogy and Geochemistry*, vol. 47. Mineralogical Society of America, Washington, D.C., 125–170. <https://doi.org/10.2138/rmg.2002.47.5>
- WIELER, R., ANDERS, E., BAUR, H., LEWIS, R.S., SIGNER, P. (1992) Characterisation of Q-gases and other noble gas components in the Murchison meteorite. *Geochimica et Cosmochimica Acta* 56, 2907–2921. [https://doi.org/10.1016/0016-7037\(92\)90367-R](https://doi.org/10.1016/0016-7037(92)90367-R)
- YOKOYAMA, T., NAGASHIMA, K., NAKAI, I., YOUNG, E.D., ABE, Y. *et al.* (2023) Samples returned from the asteroid Ryugu are similar to Ivuna-type carbonaceous meteorites. *Science* 379, eabn7850. <https://doi.org/10.1126/science.abn7850>

Dissecting the complex Ne-Ar-N signature of asteroid Ryugu by step-heating analysis

J. Gamblin, E. Füri, B. Marty, L. Zimmermann, D.V. Bekaert

Supplementary Information

The Supplementary Information includes:

- Detailed Methodology
- Figures S-1 and S-2
- Tables S-1 and S-2
- Supplementary Information References

Detailed Methodology

Ryugu sample C0015

Sample C0015 (Fig. S-1) is a single particle (1.8 ± 0.2 mg; weighed at JAXA's curation facility) that was collected during the second touchdown of JAXA's Hayabusa2 spacecraft on asteroid (162173) Ryugu and corresponds to surface or sub-surface material. It was kept under ultra-pure N₂ during weighing, storage, and shipping in a stainless-steel capsule to avoid contamination by Earth's atmosphere. At the Centre de Recherches Pétrographiques et Géochimiques (CRPG) noble gas facility, the particle was placed into a ZnSe-windowed laser chamber within a N₂-filled glove box. The isotopic composition of N₂ used for sample handling at CRPG was close to atmospheric. The sample pits were covered by a second ZnSe window to prevent the particle from bouncing out of position during laser heating and degassing. Once the chamber was connected to the purification line of the Noblesse-HR (3F4M) noble gas mass spectrometer, it was pumped to ultra-high vacuum ($\sim 10^{-9}$ bar) using a turbomolecular pump and baked at 100 °C overnight to remove any adsorbed terrestrial gases from the inner surfaces of the laser chamber and any adsorbed dry N₂ from the particle surface.

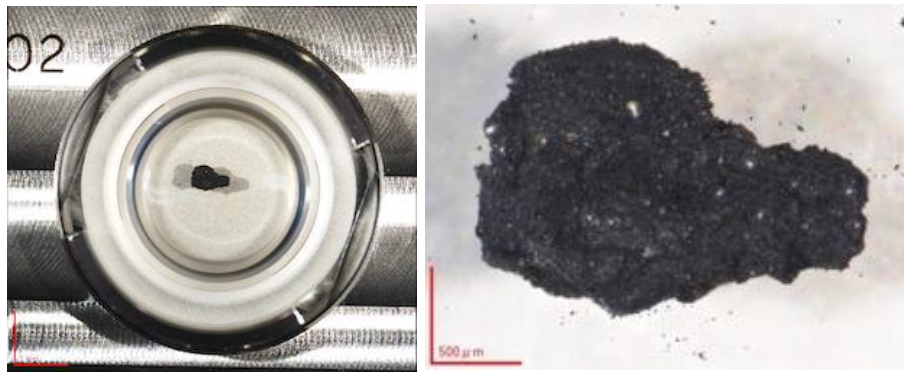


Figure S-1 Optical microscope images of particle C0015 in its sample storage dish taken at JAXA's curation facility (images from Hayabusa2, Ryugu Sample Curatorial Dataset, Institute of Space and Astronautical Science (ISAS), Japan Aerospace Exploration Agency (JAXA): <https://doi.org/10.17597/ISAS.DARTS/CUR-Ryugu-description>).

Step-heating gas extraction

Noble gases (Ne, Ar) and N were extracted under static vacuum from particle C0015 by step-heating using a 10.6 μm CO₂-laser (MIR10², Elemental Scientific) at increasing power (*i.e.* 1 to 45 % of the total power of 32 W). A total of 85 heating steps were performed, allowing the successive release of gases contained in different carrier phases. When a large amount of gas was extracted at a given laser power, further extraction steps were performed at the same power until the amount of extracted gases decreased. A high-resolution CCD video camera above the extraction chamber permitted to monitor sample heating (Fig. S-2) and melting, which was achieved at 24 % of the maximum laser power. A limitation of this method is the lack of knowledge of the heating temperature of the sample. In addition, during the extractions at high temperature, vapour deposits began to accumulate on the second window covering the sample, thus reducing the heating efficiency and the visibility of the sample. Gentle tapping against the laser chamber permitted to move the window to a clean spot. Notably, after steps #70 and #71 (at 17 % of the maximum laser power), for which the N isotope ratio was significantly lower than for the previous steps (Fig. 1c), the window was moved and the laser power lowered to 9 % to ensure that the laser beam still went through the window without loss by absorption. For the first 26 steps, the particle was heated for 4 min, whereas for the following 59 steps, the heating duration was increased to 12 min.

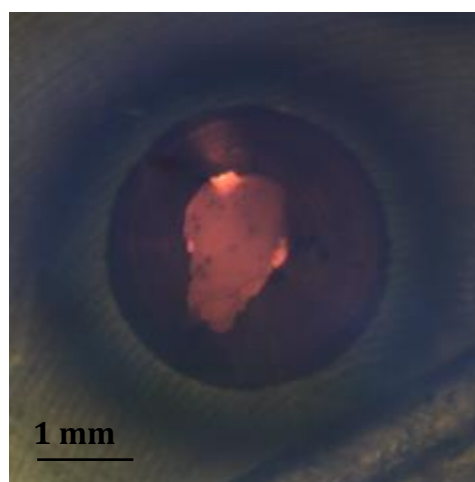


Figure S-2 Camera view of particle C0015 at heating step #73 and 15 % of the maximum laser power.

Gas purification

Following gas extraction, the gas was split into two calibrated volumes for specific noble gas (Ne, Ar) and N purifications (Zimmermann *et al.*, 2009).

Within the all-metal line used for noble gas purification, Ar was first separated from Ne by adsorption onto a charcoal finger held at $-196\text{ }^{\circ}\text{C}$ using liquid nitrogen for 5 min. Neon was then purified by exposure to a Ti-sponge getter held at $600\text{ }^{\circ}\text{C}$ for 10 min, followed by exposure to a second charcoal finger at liquid nitrogen temperature and two SAES Ti-Al getters at room temperature for 10 min. After Ne inlet into the Noblesse–HR noble gas mass spectrometer, two GP-50 SAES getters at room temperature, connected to the source and detector blocks, and an additional charcoal finger held at $-196\text{ }^{\circ}\text{C}$ were used for 10 min prior to the start of the analysis and during the entire analytical sequence to minimise contributions of $^{40}\text{Ar}^{2+}$, H_2O^+ , HF^+ , and $^{44}\text{CO}_2^{2+}$ to the $^{20,22}\text{Ne}^+$ signals and preserve a constant H_2 level.

Following the Ne analysis, Ar was desorbed from the charcoal finger and purified by exposure to the Ti-sponge getter at $600\text{ }^{\circ}\text{C}$ and the two SAES getters at room temperature for 10 min. During the Ar analysis, the two GP-50 SAES getters were used to minimise the $\text{H}^{35,37}\text{Cl}^+$ signals and maintain a constant, low H_2 level.

In parallel, N was purified within a Pyrex and quartz-glass line based on the procedure previously described by Humbert *et al.* (2000), Hashizume and Marty (2004), and Zimmermann *et al.* (2009). Nitrogen (and other species such as H, C, S) was oxidised thanks to the O_2 released during heating of CuO sticks from $450\text{ }^{\circ}\text{C}$ to $900\text{ }^{\circ}\text{C}$ for 25 min. A U-shaped cold trap at $-180\text{ }^{\circ}\text{C}$ trapped the different oxidised species except for NO_x . The CuO sticks were then gradually cooled to $800\text{ }^{\circ}\text{C}$, $700\text{ }^{\circ}\text{C}$, $600\text{ }^{\circ}\text{C}$, $500\text{ }^{\circ}\text{C}$, and $300\text{ }^{\circ}\text{C}$ (15 min for each step) to re-absorb excess O_2 (Robinson and Kusakabe, 1975) and reduce NO_x to molecular nitrogen (N_2). Once the CuO sticks reached $600\text{ }^{\circ}\text{C}$, a glass finger containing several platinum foils was cooled to $-175\text{ }^{\circ}\text{C}$ to improve the trapping efficiency of the remaining oxidised impurities. Prior to expanding N_2 into the Noblesse–HR noble gas mass spectrometer, the pressure was monitored using a hot cathode ion gauge to ensure that an appropriate amount of gas was inlet to match the $^{28}\text{N}_2^+$ signal of air standard measurements and to avoid saturation of the detectors. If required, only a fraction of the extracted and purified N_2 was inlet and analysed.

Noble gas mass spectrometry analyses

Purified gases (Ne, Ar, N_2) were analysed sequentially using a Noblesse–HR noble gas mass spectrometer (Nu Instruments) at a trap current of $150\text{ }\mu\text{A}$ and specific source settings to maximise sensitivity and minimise instrumental mass fractionation for each gas species. The three isotopes of Ne were measured simultaneously on three ion counters ($^{22}\text{Ne}^+$ on IC0, $^{21}\text{Ne}^+$ on IC2, $^{20}\text{Ne}^+$ on IC3) for 25 cycles. The $^{40}\text{Ar}^{++}$ signal was monitored during each cycle; however, given that the $^{40}\text{Ar}^{++}$ peak is partially resolved from that of $^{20}\text{Ne}^+$, no correction was applied to the $^{20}\text{Ne}^+$ signal. The $^{44}\text{CO}_2^+$ signal was also measured during each cycle by peak-jumping, and the $^{22}\text{Ne}^+$ signal was corrected using a $^{44}\text{CO}_2^{++}/^{44}\text{CO}_2^+$ ionisation ratio of 1.2 %. (The $^{44}\text{CO}_2^{++}/^{44}\text{CO}_2^+$ ionisation ratio was previously determined from background CO_2 in the mass spectrometer, and by varying the CO_2 pressure by partially closing the valve to the source getter). The $^{21}\text{Ne}^+$ signal was measured at the peak center; no hydride ($^{20}\text{NeH}^+$) correction was performed because the getter allowed maintaining a low H_2 background. After releasing Ar from the charcoal finger, the three Ar isotopes were analysed in multi-collection mode ($^{40}\text{Ar}^+$ on Fa0 with a $10^{11}\text{ }\Omega$ resistor, $^{38}\text{Ar}^+$ on IC2, $^{36}\text{Ar}^+$ on IC3) for 25 cycles. The three isotopologues of N_2 were also analysed simultaneously at mass 28 ($^{14}\text{N}^{14}\text{N}^+$) on Fa2 with a $10^{11}\text{ }\Omega$ resistor, mass 29 ($^{14}\text{N}^{15}\text{N}^+$) on Fa1 with a $10^{12}\text{ }\Omega$ resistor, and mass 30 ($^{15}\text{N}^{15}\text{N}^+$) on IC0, after measuring the $^{12,13}\text{C}^{16}\text{O}^+$ signals by changing the voltage of the LIN2 lense. Following data acquisition, which comprised 25 measurement cycles, the $^{14}\text{N}^{14}\text{N}^+$ and $^{14}\text{N}^{15}\text{N}^+$ signals were obtained by correcting for the $^{12}\text{C}^{16}\text{O}^+$ and $^{13}\text{C}^{16}\text{O}^+$ contributions, respectively.

Measured ion signals were processed using the “Nu Instruments Calculation Editor” (NICE); detector baselines and contributions from interfering species were subtracted from the signals of interest, and isotope ratios were calculated for each measurement cycle. The “Nu Noble” software was then used to extrapolate the corrected ion signals and isotope ratios to $t = 0$ using a linear (for Ne and Ar) or exponential equation (for N₂). Baseline- and interference-corrected Ne, Ar, and N₂ ion signals, as well as ²⁰Ne/²²Ne, ²¹Ne/²²Ne, ⁴⁰Ar/³⁶Ar, ³⁸Ar/³⁶Ar, ²⁸N₂/²⁹N₂, and ²⁹N₂/³⁰N₂ ratios, extrapolated to $t = 0$, are available for download at <https://doi.org/10.24396/ORDAR-144>.

To determine the analytical sensitivity and the instrumental mass fractionation of the Noblesse–HR noble gas mass spectrometer, purified air standard aliquots were analysed at least twice a week for Ne, Ar, and N₂. The reproducibility of air standard measurements was 2.1 % for ²⁰Ne, 1.5 % for ³⁶Ar, and 4.5 % for ²⁸N₂ abundances, and 0.59 % for ²⁰Ne/²²Ne, 1.77 % for ²¹Ne/²²Ne, 0.20 % for ³⁸Ar/³⁶Ar, and 0.07% for ²⁸N₂/²⁹N₂ isotope ratios over the 20-week measurement period. Noble gas (Ne, Ar) and N₂ abundances were calculated based on the sensitivity of the mass spectrometer using equation S-1 (Zimmermann and Bekaert, 2020):

$$n = \frac{U \times V_I}{R \times S \times d \times 760 \times V_M} \quad \text{Eq. S-1,}$$

where n is the abundance (mol), U is the ion signal (V), V_I is the volume of the laser chamber (24.35 cm³), R is the resistance at the collector outlet (10¹¹ or 10¹² Ω), S is the sensitivity (4.9 ± 0.1 × 10⁻⁵ A/Torr for ²⁰Ne, 2.26 ± 0.03 × 10⁻⁴ A/Torr for ³⁶Ar, and 1.30 ± 0.06 × 10⁻⁴ A/Torr for ²⁸N₂, on average), d is the dilution coefficient, and V_M is the molar volume (22,414 cm³/mol). Procedural blanks (laser off) for a 4 min-long extraction were 1.8 ± 0.2 × 10⁻¹⁶ mol ²⁰Ne, 1.2 ± 0.1 × 10⁻¹⁷ mol ³⁶Ar, and 4.5 ± 1.4 × 10⁻¹² mol ²⁸N₂, and 3.3 ± 0.3 × 10⁻¹⁶ mol ²⁰Ne, 1.4 ± 0.2 × 10⁻¹⁷ mol ³⁶Ar, and 3.8 ± 1.3 × 10⁻¹² mol ²⁸N₂ for a 12 min-long extraction.

Blank-corrected Ne, Ar, and N₂ abundances (in mol), and ²⁰Ne/²²Ne, ²¹Ne/²²Ne, ³⁸Ar/³⁶Ar, and δ¹⁵N values corrected for instrumental mass fractionation, for the 85 extraction steps of particle C0015, as well as calculated bulk abundances and isotope ratios, are available for download at <https://doi.org/10.24396/ORDAR-144>. Uncertainties of blank-corrected Ne, Ar, and N₂ abundances and isotopic ratios were calculated using the Monte Carlo method. Isotope ratios of heating-steps with ≥30 % blank contributions are excluded from the figures and further discussions. Nitrogen isotope ratios are given in the δ¹⁵N notation:

$$\delta^{15}\text{N} (\text{‰}) = \left(\frac{1 + 2 \times (^{28}\text{N}_2/^{29}\text{N}_2)_{\text{atm}}}{1 + 2 \times (^{28}\text{N}_2/^{29}\text{N}_2)_{\text{measured}}} - 1 \right) \times 1000 \quad \text{Eq. S-2,}$$

where (²⁸N₂/²⁹N₂)_{atm} is the isotopic composition of atmospheric N₂ (136.05; Nier, 1950).

Table S-1 Calculated bulk Ne-Ar-N concentrations and isotope ratios of Ryugu particle C0015. Uncertainties on the abundance-weighted average values (1σ) were calculated using a Monte Carlo method. Uncertainties of noble gas and N concentrations are mainly controlled by the uncertainty on the sample mass.

²⁰ Ne (mol/g)	²⁰ Ne/ ²² Ne	³⁶ Ar (mol/g)	³⁸ Ar/ ³⁶ Ar	N (ppm)	δ ¹⁵ N (‰)
2.13 ± 0.23 × 10 ⁻⁹	13.07 ± 0.02	1.80 ± 0.20 × 10 ⁻¹⁰	0.1865 ± 0.0001	1760 ± 195	+24.43 ± 0.17

Nitrogen components in CI chondrites and Ryugu

Several previous studies have attempted to dissect the different N components and their isotopic compositions in CI chondrites and Ryugu samples. High-resolution stepped combustion analyses of Orgueil chips revealed that most of the N in CIs is released at temperatures between 400 °C and 600 °C due to the combustion of organic matter (*e.g.*, Grady *et*

al., 2002; Sephton *et al.*, 2003). Nanodiamonds also contribute to the N release within this temperature range, whereas graphite and silicon carbides have higher combustion temperatures of 500 to 700 °C and 1200 to 1600 °C, respectively (Sephton *et al.*, 2003, and references therein). The heterogeneous distribution of N-bearing components in carbonaceous chondrites (*e.g.*, Kerridge, 1985) and Ryugu samples (Nakamura *et al.*, 2022) has also been highlighted. Notably, ¹⁵N-hotspots ($\delta^{15}\text{N}$ up to +3000 ‰) and ¹⁵N-coldspots ($\delta^{15}\text{N}$ down to –150 ‰), identified by *in situ* secondary ion mass spectrometry analyses, were inferred to control the bulk $\delta^{15}\text{N}$ variations detected in Ryugu particles by the Phase-2 curation team (Institute for Planetary Materials, Okayama University; Nakamura *et al.*, 2022).

The predominant N-bearing phase in CIs is insoluble organic matter (IOM) (Matsumoto *et al.*, 2024), which has a $\delta^{15}\text{N}$ value of about +31 ‰ (Alexander *et al.*, 2007). Given that IOM is sensitive to brief thermal events such as solar heating and impacts (Quirico *et al.*, 2018), the N signature of this component may have been modified by regolith processes at Ryugu's surface. Nonetheless, the N isotope ratios of insoluble carbonaceous residues of Ryugu are close to the IOM value (+17.4 ± 1.9 ‰ and +30 ± 4.3 ‰ in two different samples; Yabuta *et al.*, 2023). Other N-bearing phases can show highly variable $\delta^{15}\text{N}$ values. For example, the $\delta^{15}\text{N}$ values of C-rich exogenous clasts in Ryugu samples vary from –505 ± 149 ‰ to +3219 ± 672 ‰ (Nguyen *et al.*, 2023). Furthermore, Barosch *et al.* (2022) and Nguyen *et al.* (2023) identified various types of presolar grains in Ryugu material, such as presolar oxides, silicates, silicon carbide (SiC), graphite, and C-anomalous organics, which are known to show a wide range of $\delta^{15}\text{N}$ values inherited from their different stellar sources (*e.g.*, –825 ± 189 ‰ to +705 ± 428 ‰ for SiC and –536 ± 465 ‰ to +1512 ± 221 ‰ for presolar graphite and SiC; Nguyen *et al.*, 2023). The N isotopic composition of presolar nanodiamonds, the carrier phase of Ne-HL, could not be determined in Ryugu samples due to their small size (Barosch *et al.*, 2022); however, previous measurements in primitive chondrites revealed that they contain abundant N with strikingly negative $\delta^{15}\text{N}$ values down to –348 ± 7 ‰ (Russell *et al.*, 1996). It is noteworthy that the isotopic composition of N in phase Q is poorly known due to impossibility of isolating pure Q; based on stepped combustion analyses of carbonaceous chondrites, Verchovsky (2017) argued that phase Q carries isotopically light N with a $\delta^{15}\text{N}$ value <–150 ‰ and possibly similar to the solar value (*i.e.* $\delta^{15}\text{N}_{\text{Sun}} = -383 \pm 8$ ‰; Marty *et al.*, 2011) (Verchovsky, 2017). All of the aforementioned N-bearing phases (*i.e.* organics, various presolar phases, phase Q) – as well as nitrides (Matsumoto *et al.*, 2024) and NH-rich compounds (Pilorget *et al.*, 2022) – are likely present in Ryugu particle C0015 and contribute to the $\delta^{15}\text{N}$ variations observed during step-heating analysis.

Table S-2 Nitrogen abundance and isotopic composition ($\delta^{15}\text{N}$) of CI chondrites and Ryugu samples.

Sample	N (ppm)	$\delta^{15}\text{N}$ (‰)	Reference
Alais (CI1)	1250	+31	Kerridge (1985)
	1900	+45.7	Pearson <i>et al.</i> (2006)
	1800	+41.8	Pearson <i>et al.</i> (2006)
	2400	+61.1	Pearson <i>et al.</i> (2006)
	2100	+56.5	Pearson <i>et al.</i> (2006)
	1800	+54.7	Pearson <i>et al.</i> (2006)
Ivuna (CI1)	1855	+52	Kerridge (1985)
	2070	+44.9	Alexander <i>et al.</i> (2012)
	1113.42 ± 36.26	+36.4 ± 0.4	Hashizume <i>et al.</i> (2024)
Orgueil (CI1)	1476	+46.2	Injerd and Kaplan (1974)
	1360	+39	Robert and Epstein (1982)
	1999.6	+32	Grady <i>et al.</i> (2002)
	2070	+32.2	Sephton <i>et al.</i> (2003)
	5600	+38.0	Pearson <i>et al.</i> (2006)
	8200	+41.4	Pearson <i>et al.</i> (2006)
	2100	+54.2	Pearson <i>et al.</i> (2006)
	1490	+44.1	Alexander <i>et al.</i> (2012)
	2080	+35.9	Alexander <i>et al.</i> (2012)

Y-980115 (CI1 or CY)	900 438	−2.8 +4.0 ± 0.3	Chan <i>et al.</i> (2016) Hashizume <i>et al.</i> (2024)
Ryugu A0022	1170	+40.53	Nakamura <i>et al.</i> (2022)
Ryugu A0033	1660	+17.82	Nakamura <i>et al.</i> (2022)
Ryugu A0035	1930	+52.08	Nakamura <i>et al.</i> (2022)
Ryugu A0048	1290	+35.00	Nakamura <i>et al.</i> (2022)
Ryugu A0073	1930	+52.34	Nakamura <i>et al.</i> (2022)
Ryugu A0078	1810	+50.94	Nakamura <i>et al.</i> (2022)
Ryugu C0008	1590	+46.23	Nakamura <i>et al.</i> (2022)
Ryugu C0019	1010	+26.80	Nakamura <i>et al.</i> (2022)
Ryugu C0027	1030	+22.66	Nakamura <i>et al.</i> (2022)
Ryugu C0079	1070	+22.85	Nakamura <i>et al.</i> (2022)
Ryugu C0081	2160	+53.01	Nakamura <i>et al.</i> (2022)
Ryugu C0082	1910	+0.37	Nakamura <i>et al.</i> (2022)
Ryugu A0106 #1	1600	+39.1	Naraoka <i>et al.</i> (2023)
Ryugu A0106 #2	1700	+53.2	Naraoka <i>et al.</i> (2023)
Ryugu A0106 #3	1600	+36.7	Naraoka <i>et al.</i> (2023)
Ryugu C0107 #2	1300	+39.0	Oba <i>et al.</i> (2023)
Ryugu C0107 #3	1400	+32.6	Oba <i>et al.</i> (2023)
Ryugu C0107 #4	1500	+38.8	Oba <i>et al.</i> (2023)
Ryugu A0105-05*	884.03 ± 24.59	+18.14 ± 0.94	Broadley <i>et al.</i> (2023)
Ryugu C0106-06*	855.62 ± 10.34	+19.47 ± 0.89	Broadley <i>et al.</i> (2023)
Ryugu A0105-07*	524.44 ± 19.46	+1.7 ± 0.5	Hashizume <i>et al.</i> (2024)
Ryugu C0106-07*	616.56 ± 17.36	+0.2 ± 0.6	Hashizume <i>et al.</i> (2024)

* Pelletised samples analysed by the Hayabusa2-initial-analysis volatile team

Supplementary Information References

- Alexander, C.M.O'D., Fogel, M., Yabuta, H., Cody, G.D. (2007) The origin and evolution of chondrites recorded in the elemental and isotopic compositions of their macromolecular organic matter. *Geochimica et Cosmochimica Acta* 71, 4380–4403. <https://doi.org/10.1016/j.gca.2007.06.052>
- Alexander, C.M.O'D., Bowden, R., Fogel, M.L., Howard, K.T., Herd, C.D.K., Nittler, L.R. (2012) The provenances of asteroids, and their contributions to the volatile inventories of the terrestrial planets. *Science* 337, 721–723. <https://doi.org/10.1126/science.1223474>
- Barosch, J., Nittler, L.R., Wang, J., Alexander, C.M.O'D., De Gregorio, B.T. *et al.* (2022) Presolar stardust in asteroid Ryugu. *The Astrophysical Journal Letters* 935, L3. <https://doi.org/10.3847/2041-8213/ac83bd>
- Broadley, M.W., Byrne, D.J., Füri, E., Zimmermann, L., Marty, B. *et al.* (2023) The noble gas and nitrogen relationship between Ryugu and carbonaceous chondrites. *Geochimica et Cosmochimica Acta* 345, 62–74. <https://doi.org/10.1016/j.gca.2023.01.020>
- Chan, Q.H.S., Chikaraishi, Y., Takano, Y., Ogawa, N.O., Ohkouchi, N. (2016) Amino acid compositions in heated carbonaceous chondrites and their compound-specific nitrogen isotopic ratios. *Earth, Planets and Space* 68, 7. <https://doi.org/10.1186/s40623-016-0382-8>
- Grady, M.M., Verchovsky, A.B., Franchi, I.A., Wright, I.P., Pillinger, C.T. (2002) Light element geochemistry of the Tagish Lake CI2 chondrite: Comparison with CI1 and CM2 meteorites. *Meteoritics & Planetary Science* 37, 713–735. <https://doi.org/10.1111/j.1945-5100.2002.tb00851.x>

- Hashizume, K., Marty, B. (2004) Nitrogen isotopic analyses at the sub-picomole level using an ultralow blank laser extraction technique. In: de Groot, P.A. (Ed.) *Handbook of Stable Isotope Analytical Techniques, vol. 1*. Elsevier, Amsterdam, 361–374. <https://doi.org/10.1016/B978-044451114-0/50019-3>
- Hashizume, K., Ishida, A., Chiba, A., Okazaki, R., Yogata, K., Yada, T., Kitajima, F., Yurimoto, H., Nakamura, T., Noguchi, T., Yabuta, H., Naraoka, H., Takano, Y., Sakamoto, K., Tachibana, S., Nishimura, M., Nakato, A., Miyazaki, A., Abe, M., Okada, T., Usui, T., Yoshikawa, M., Saiki, T., Terui, F., Tanaka, S., Nakazawa, S., Watanabe, S.-i., Tsuda, Y., Broadley, M.W., Busemann, H. and the Hayabusa2 Initial Analysis Volatile Team. (2024) The Earth atmosphere-like bulk nitrogen isotope composition obtained by stepwise combustion analyses of Ryugu return samples. *Meteoritics & Planetary Science*. <https://doi.org/10.1111/maps.14175>
- Humbert, F., Libourel, G., France-Lanord, C., Zimmermann, L., Marty, B. (2000) CO₂-laser extraction-static mass spectrometry analysis of ultra-low concentrations of nitrogen in silicates. *Geostandards Newsletter* 24, 255–260. <https://doi.org/10.1111/j.1751-908X.2000.tb00777.x>
- Injerd, W.G., Kaplan, I.R. (1974) Nitrogen isotope distribution in meteorites. *Meteoritics* 9, 352.
- Kerridge, J.F. (1985) Carbon, hydrogen and nitrogen in carbonaceous chondrites: Abundances and isotopic compositions in bulk samples. *Geochimica et Cosmochimica Acta* 49, 1707–1714. [https://doi.org/10.1016/0016-7037\(85\)90141-3](https://doi.org/10.1016/0016-7037(85)90141-3)
- Matsumoto, T., Noguchi, T., Miyake, A., Igami, Y., Haruta, M. *et al.* (2024) Influx of nitrogen-rich material from the outer Solar System indicated by iron nitride in Ryugu samples. *Nature Astronomy* 8, 207–215. <https://doi.org/10.1038/s41550-023-02137-z>
- Nakamura, E., Kobayashi, K., Tanaka, R., Kunihiro, T., Kitagawa, H. *et al.* (2022) On the origin and evolution of the asteroid Ryugu: A comprehensive geochemical perspective. *Proceedings of the Japan Academy, Series B* 98, 227–282. <https://doi.org/10.2183/pjab.98.015>
- Naraoka, H., Takano, Y., Dworkin, J.P., Oba, Y., Hamase, K. *et al.* (2023) Soluble organic molecules in samples of the carbonaceous asteroid (162173) Ryugu. *Science* 379, eabn9033. <https://doi.org/10.1126/science.abn9033>
- Nguyen, A.N., Mane, P., Keller, L.P., Piani, L., Abe, Y. *et al.* (2023) Abundant presolar grains and primordial organics preserved in carbon-rich exogenous clasts in asteroid Ryugu. *Science Advances* 9, eadh1003. <https://doi.org/10.1126/sciadv.adh1003>
- Nier, A.O. (1950) A redetermination of the relative abundances of the isotopes of carbon, nitrogen, oxygen, argon, and potassium. *Physical Review* 77, 789–793. <https://doi.org/10.1103/PhysRev.77.789>
- Oba, Y., Koga, T., Takano, Y., Ogawa, N.O., Ohkouchi, N. *et al.* (2023) Uracil in the carbonaceous asteroid (162173) Ryugu. *Nature Communications* 14, 1292. <https://doi.org/10.1038/s41467-023-36904-3>
- Pearson, V.K., Sephton, M.A., Franchi, I.A., Gibson, J.M., Gilmour, I. (2006) Carbon and nitrogen in carbonaceous chondrites: Elemental abundances and stable isotopic compositions. *Meteoritics & Planetary Science* 41, 1899–1918. <https://doi.org/10.1111/j.1945-5100.2006.tb00459.x>
- Pilorget, C., Okada, T., Hamm, V., Brunetto, R., Yada, T. *et al.* (2022) First compositional analysis of Ryugu samples by the MicrOmega hyperspectral microscope. *Nature Astronomy* 6, 221–225. <https://doi.org/10.1038/s41550-021-01549-z>
- Quirico, E., Bonal, L., Beck, P., Alexander, C.M.O'D., Yabuta, H., Nakamura, T., Nakato, A., Flandinet, L., Montagnac, G., Schmitt-Kopplin, P., Herd, C.D.K. (2018) Prevalence and nature of heating processes in CM and C2-ungrouped chondrites as revealed by insoluble organic matter. *Geochimica et Cosmochimica Acta* 241, 17–37. <https://doi.org/10.1016/j.gca.2018.08.029>
- Robert, F., Epstein S. (1982) The concentration and isotopic composition of hydrogen, carbon and nitrogen in carbonaceous meteorites. *Geochimica et Cosmochimica Acta* 46, 81–89. [https://doi.org/10.1016/0016-7037\(82\)90293-9](https://doi.org/10.1016/0016-7037(82)90293-9)
- Robinson, B.W., Kusakabe, M. (1975) Quantitative preparation of sulfur dioxide, for ³⁴S/³²S analyses, from sulfides by combustion with cuprous oxide. *Analytical Chemistry* 47, 1179–1181. <https://doi.org/10.1021/ac60357a026>

- Russell, S.S., Arden, J.W., Pillinger, C.T. (1996) A carbon and nitrogen isotope study of diamond from primitive chondrites. *Meteoritics & Planetary Science* 31, 343–355. <https://doi.org/10.1111/j.1945-5100.1996.tb02071.x>
- Sephton, M.A., Verchovsky, A.B., Bland, P.A., Gilmour, I., Grady, M.M., Wright, I.P. (2003) Investigating the variations in carbon and nitrogen isotopes in carbonaceous chondrites. *Geochimica et Cosmochimica Acta* 67, 2093–2108. [https://doi.org/10.1016/S0016-7037\(02\)01320-0](https://doi.org/10.1016/S0016-7037(02)01320-0)
- Verchovsky, A.B. (2017) Origin of isotopically light nitrogen in meteorites. *Geochemistry International* 55, 957–970. <https://doi.org/10.1134/S0016702917110106>
- Yabuta, H., Cody, G.D., Engrand, C., Kebukawa, Y., De Gregorio, B. *et al.* (2023) Macromolecular organic matter in samples of the asteroid (162173) Ryugu. *Science* 379, eabn9057. <https://doi.org/10.1126/science.abn9057>
- Zimmermann, L., Burnard, P., Marty, B., Gaboriaud, F. (2009) Laser Ablation (193 nm), Purification and Determination of Very Low Concentrations of Solar Wind Nitrogen Implanted in Targets from the GENESIS Spacecraft. *Geostandards and Geoanalytical Research* 33, 183–194. <https://doi.org/10.1111/j.1751-908X.2009.00021.x>
- Zimmermann, L., Bekaert, D. (2020) Analyse des gaz rares par spectrométrie de masse statique - Mesures et applications. *Techniques de l'ingénieur J6637 v1*. <https://doi.org/10.51257/a-v1-j6637>